

~~NO-0177 185~~

PERFORMANCE OF TWO COUPLED LASERS(U) AEROSPACE CORP EL 1/1
SEGUNDO CA AEROPHYSICS LAB H NIRELS 05 FEB 87
TR-0086(6907)-1 SD-TR-86-96 F04701-85-C-0086

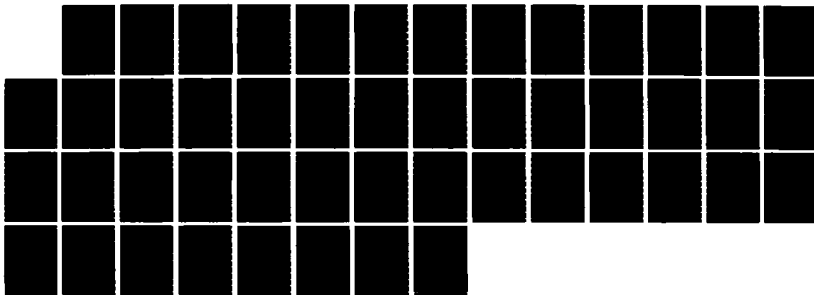
SEGUNDO CA AEROPHYSICS LAB H NIRELS 05 FEB 87

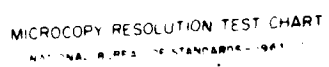
TR-0086(6907)-1 SD-TR-86-96 F04701-85-C-0086

UNCLASSIFIED

F/G 20/5

ML





MICROCOPY RESOLUTION TEST CHART
NATIONAL BUREAU OF STANDARDS - 1963-A

12

REPORT SD-TR-86-96

AD-A11185

Performance of Two Coupled Lasers

H. MIRELS
Aerophysics Laboratory
Laboratory Operations
The Aerospace Corporation
El Segundo, CA 90245

5 February 1987

APPROVED FOR PUBLIC RELEASE:
DISTRIBUTION UNLIMITED

Prepared for
SPACE DIVISION
AIR FORCE SYSTEMS COMMAND
Los Angeles Air Force Station
P.O. Box 92960, Worldway Postal Center
Los Angeles, CA 90009-2960


2

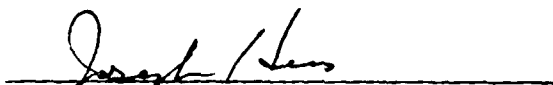
This report was submitted by The Aerospace Corporation, El Segundo, CA 90245, under Contract No. F04701-85-C-0086-P00016 with the Space Division, P.O. Box 92960, Worldway Postal Center, Los Angeles, CA 90009-2960. It was reviewed and approved for The Aerospace Corporation by W. P. Thompson, Director, Aerophysics Laboratory.

Lt Scott W. Levinson/YNS was the project officer.

This report has been reviewed by the Public Affairs Office (PAS) and is releasable to the National Technical Information Service (NTIS). At NTIS, it will be available to the general public, including foreign nationals.

This technical report has been reviewed and is approved for publication. Publication of this report does not constitute Air Force approval of the report's findings or conclusions. It is published only for the exchange and stimulation of ideas.


SCOTT W. LEVINSON, Lt, USAF
MOIE Project Officer
SD/YNS


JOSEPH HESS, GM-15
Director, AFSTC West Coast Office
AFSTC/WCO OL-AB

UNCLASSIFIED

SECURITY CLASSIFICATION OF THIS PAGE (When Data Entered)

REPORT DOCUMENTATION PAGE		READ INSTRUCTIONS BEFORE COMPLETING FORM
1. REPORT NUMBER SD-TR-86-96	2. GOVT ACCESSION NO.	3. RECIPIENT'S CATALOG NUMBER
4. TITLE (and Subtitle) PERFORMANCE OF TWO COUPLED LASERS		5. TYPE OF REPORT & PERIOD COVERED TR-0086(6907)-1
		6. PERFORMING ORG. REPORT NUMBER
7. AUTHOR(s) Harold Mirels		8. CONTRACT OR GRANT NUMBER(s) F04701-85-C-0086-P00016
9. PERFORMING ORGANIZATION NAME AND ADDRESS The Aerospace Corporation El Segundo, CA 90278		10. PROGRAM ELEMENT, PROJECT, TASK AREA & WORK UNIT NUMBERS
11. CONTROLLING OFFICE NAME AND ADDRESS Space Division Los Angeles Air Force Station Los Angeles, CA 90009		12. REPORT DATE 5 February 1987
		13. NUMBER OF PAGES 42
14. MONITORING AGENCY NAME & ADDRESS (if different from Controlling Office)		15. SECURITY CLASS. (of this report) Unclassified
		15a. DECLASSIFICATION/DOWNGRADING SCHEDULE
16. DISTRIBUTION STATEMENT (of this Report) Approved for public release; distribution unlimited.		
17. DISTRIBUTION STATEMENT (of the abstract entered in Block 20, if different from Report)		
18. SUPPLEMENTARY NOTES		
19. KEY WORDS (Continue on reverse side if necessary and identify by block number) Lasers Coupled lasers Single line performance Multi line performance Stability		
20. ABSTRACT (Continue on reverse side if necessary and identify by block number) The theory of Spencer and Lamb for the performance of two coupled lasers is generalized to account for intercavity phase shifts (transmitted wave minus reflected wave) other than $\pm \pi/2$. The results are directly applicable for the case of two coupled single line Fabry-Perot resonators with intercavity losses. Analytic expressions are given for steady-state performance and for the regions of stable operation. It is concluded that it is generally not possible to achieve stable operation on all potential laser lines for two multiline coupled lasers. Competition between stable and unstable lasing		

DD FORM 1473
(FACSIMILE)

UNCLASSIFIED

SECURITY CLASSIFICATION OF THIS PAGE (When Data Entered)

UNCLASSIFIED

SECURITY CLASSIFICATION OF THIS PAGE(When Data Entered)

19. KEY WORDS (Continued)

20. ABSTRACT (Continued)

modes, in these devices, may result in stable operations on a reduced number of lines.

UNCLASSIFIED

SECURITY CLASSIFICATION OF THIS PAGE(When Data Entered)

PREFACE

The author is indebted to Karen L. Foster for numerical support.

Accession For	
NTIS	<input checked="" type="checkbox"/>
DTIC	<input checked="" type="checkbox"/>
Uncl. Sec.	<input type="checkbox"/>
Distribution	
For	
Distribution of	
Approved by C. Sec	
by name/or	
Dist	General
A-1	



CONTENTS

PREFACE.....	1
I. INTRODUCTION.....	9
II. THEORY.....	11
A. Resonator Properties.....	11
B. Unsteady Resonator Equations.....	15
C. Steady-State Solution.....	16
D. Stability Criterion.....	18
E. Similitude.....	20
F. Beam Combination.....	20
III. SPECIAL CASES.....	25
A. Assumptions.....	25
B. Case $\cos(\phi + \psi) = \cos(\phi - \psi)$	26
C. Case $\phi^2 \ll 1$	30
IV. RESULTS AND DISCUSSION.....	33
A. ϕ Fixed and ψ Varied.....	39
B. ψ Fixed and ϕ Varied.....	39
C. Gain Medium Effects.....	39
V. MULTILINE COUPLED RESONATOR PERFORMANCE.....	41
VI. CONCLUDING REMARKS.....	43
REFERENCES.....	45
APPENDIX: ETALON PERFORMANCE.....	47

FIGURES

1. Fabry-Perot Coupled Resonator Configuration.....	12
2. Vector Sum of Electric Fields at M_{12} and M_{21}	13
3. Applications of Coupled Resonator Output.....	21
4. Effect of Saturation on Range of Ψ for Stable Operation.....	31

TABLES

I.	Coefficients that Define Gain Medium Saturation from Ref. 2.....	17
II.	Input for Numerical Computations.....	34
III.	Coupled Resonator Performance for Case of Homogeneous Medium.....	35
IV.	Coupled Resonator Performance for Case of Inhomogeneous Medium.....	37

I. INTRODUCTION

We consider two nearly identical Fabry-Perot laser oscillators, which are coupled by partial injection of the output of one laser into the second and vice versa. Spencer and Lamb¹ have shown that, under some circumstances, a steady-state solution can be obtained where the two lasers are locked to a fixed frequency and phase relation. This technique can then be used to obtain the coherent combination of the output from the two lasers.

In the theory of Spencer and Lamb, it is assumed that there is a fixed phase difference (herein denoted $\psi = -\pi/2$) between the transmitted and reflected radiation at the coupling mirrors. This boundary condition is appropriate when the coupling mirrors are equivalent to a lossless Fabry-Perot etalon (see Appendix). A more general treatment is to consider the value of ψ to be arbitrary. This approach is used herein.

The equations that describe the performance of coupled laser oscillators operating on a single frequency are first noted. Weak coupling is assumed. A third-order saturation model² is used for both homogeneous and inhomogeneous laser media. Analytic and numerical solutions are then obtained for special cases with emphasis on the stability range for steady-state operation. Finally, the stability of multiline coupled oscillators is discussed.

II. THEORY

Equations that define the performance of single line coupled resonators are deduced herein.

A. RESONATOR PROPERTIES

Coupled resonators are illustrated in Fig. 1a. The coupling occurs through mirrors M_{12} and M_{21} . The electric field at these mirrors is noted in Fig. 1b. The reflected electric field at M_{12} and M_{21} is denoted $E_1 e^{i\phi_1}$ for M_{12} and $E_2 e^{i\phi_2}$ for M_{21} . The corresponding transmitted electric field in M_{12} and M_{21} is $(T/R)^{1/2} E_2 e^{i(\phi_2 + \psi)}$ and $(T/R)^{1/2} E_1 e^{i(\phi_1 + \psi)}$. Here, T and R represent net intensity transmission and reflection coefficients while $\psi \equiv \phi^t - \phi^r$ is the net phase difference between the transmitted and reflected waves. Values of T , R , and ψ are given in the Appendix for cases where mirrors M_{12} and M_{21} form a Fabry-Perot etalon. When there are no losses, $T + R = 1$ and $\psi = \pm \pi/2$. The latter result is consistent with assumptions in Ref. 1. However, when losses occur, $T + R < 1$ and ψ depends on the optical path length $2\pi h/\lambda$ (Appendix). Hence, consideration is given herein of cases for which $|\psi| \neq \pi/2$.

Vector addition of the reflected and transmitted wave in each resonator (Fig. 2) provides the net perturbation, per round trip, caused by the injection process. For weak coupling, $(T/R)^{1/2} \ll 1$, the result is

$$\Delta E_1 = (T/R)^{1/2} E_2 \cos(\phi + \psi) \quad (1a)$$

$$\Delta \phi_1 = (T/R)^{1/2} (E_2/E_1) \sin(\phi + \psi) \quad (1b)$$

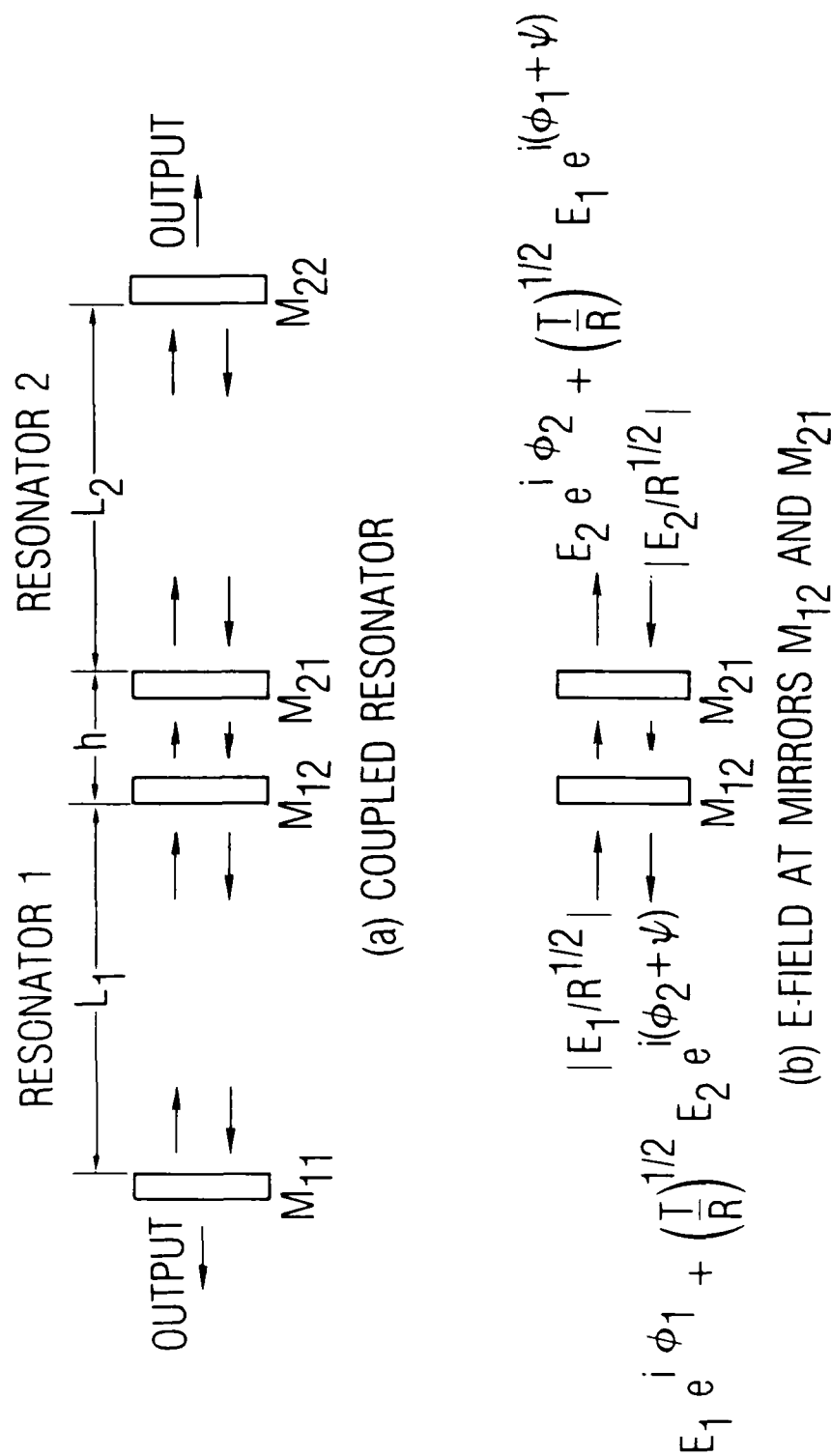
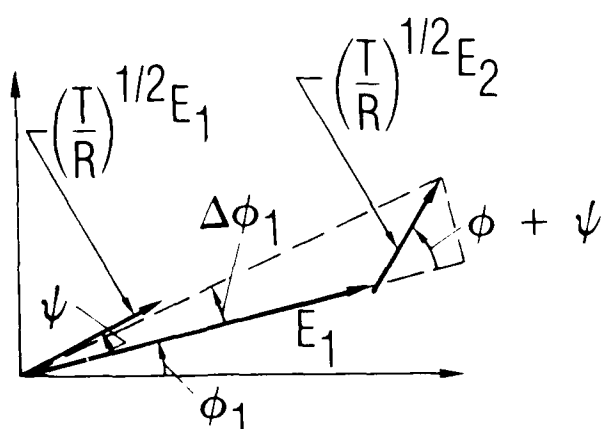
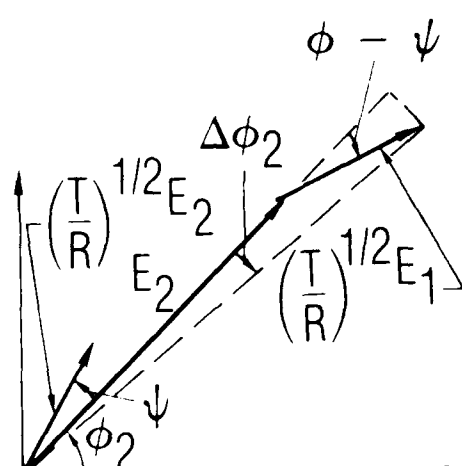


Fig. 1. Fabry-Perot coupled resonator configuration.

$$\phi \equiv \phi_2 - \phi_1$$



(a) E_1 FIELD



(b) E_2 FIELD

Fig. 2. Vector sum of electric fields at M_{12} and M_{21} .

$$\Delta E_2 = (T/R)^{1/2} E_1 \cos (\phi - \psi) \quad (1c)$$

$$\Delta \phi_2 = -(T/R)^{1/2} (E_1/E_2) \sin (\phi - \psi) \quad (1d)$$

where $\phi = \phi_2 - \phi_1$. The round-trip time in each resonator is

$$t_{r,n} = 2 L_n / c \quad (2)$$

where $n = 1, 2$. The empty cavity resonance frequency for each resonator is

$$\Omega_1 = (2\pi N_1 - \phi_1)(c/2L_1) \quad (3a)$$

$$\Omega_2 = (2\pi N_2 - \phi_2)(c/2L_2) \quad (3b)$$

where N_1 and N_2 are integers. Here, ϕ_1 and ϕ_2 denote the net phase change induced by reflections during a round trip within resonators 1 and 2, respectively. Both homogeneous and inhomogeneous media are considered. For later reference, we introduce the normalized frequency relations

$$\xi = (\omega - \nu) / \gamma \quad (4a)$$

$$\Delta_n = (\omega - \Omega_n) / \gamma \quad (4b)$$

$$\Delta = \Delta_2 - \Delta_1 = (\Omega_1 - \Omega_2) / \gamma \quad (4c)$$

where ω , ν , and γ denote line center frequency, laser frequency, and homogeneous line width (HWHM), respectively.

B. UNSTEADY RESONATOR EQUATIONS

Single-mode operation of a Fabry-Perot resonator has been described by Lamb.² These equations can be generalized to the case of two coupled resonators by inclusion of Eqs. (1a) through (1d). The result is

$$\frac{dE_1}{dt} = (a_1 - \beta_1 I_1) E_1 + M_1 E_2 \cos(\phi + \psi) \quad (5a)$$

$$\frac{dE_2}{dt} = (a_2 - \beta_2 I_2) E_2 + M_2 E_1 \cos(\phi - \psi) \quad (5b)$$

$$\frac{d\phi_1}{dt} = \gamma(\xi - \Delta_1) + \sigma_1 - \rho_1 I_1 + M_1 (E_2/E_1) \sin(\phi + \psi) \quad (5c)$$

$$\frac{d\phi_2}{dt} = \gamma(\xi - \Delta_2) + \sigma_2 - \rho_2 I_2 - M_2 (E_1/E_2) \sin(\phi - \psi) \quad (5d)$$

$$\begin{aligned} \frac{d\phi}{dt} = & -\gamma\Delta + \sigma_2 - \sigma_1 + \rho_1 I_1 - \rho_2 I_2 - M_2 (E_1/E_2) \sin(\phi - \psi) \\ & - M_1 (E_2/E_1) \sin(\phi + \psi) \end{aligned} \quad (5e)$$

where $I_n = E_n^2$ and

$$M_n = (T/R)^{1/2} / t_{r,n} \quad (6)$$

The last term on the right hand side of Eqs. (5a) through (5d) is deduced by dividing Eqs. (1a) through (1d) by $t_{r,n}$ to obtain the rate of change per unit time.

The quantities a_n , β_n , σ_n , ρ_n are functions of ξ and resonator parameters $F_{1,n}$, $F_{2,n}$, and $F_{3,n}$ as defined in Table I. When $\psi = -\pi/2$, Eqs. (5a) through (5e) agree with the corresponding equations in Ref. 1 except for the saturation model, which herein is limited to the third-order (in E) theory of Lamb. The third-order theory is accurate² for $1 < F_{1,n}/F_{2,n} \lesssim 1.2$ (denoted N/N_T in Ref. 2), but is expected to give qualitatively correct results for larger values of this parameter.

C. STEADY-STATE SOLUTION

A steady-state solution of Eqs. (5a) through (5e) is obtained by assuming that the time derivative terms are zero. The resulting equations can be put in the form

$$\frac{I_1}{I_2} = \frac{\beta_2 [a_1 + M_1 (I_2/I_1)^{1/2} \cos(\phi + \psi)]}{\beta_1 [a_2 + M_2 (I_1/I_2)^{1/2} \cos(\phi - \psi)]} \quad (7a)$$

$$\xi = \frac{\gamma \Delta_1 - M_1 (I_2/I_1)^{1/2} \sin(\phi + \psi)}{\gamma + (\sigma_1/\xi) - (\rho_1/\xi \beta_1) [a_1 + M_1 (I_2/I_1)^{1/2} \cos(\phi + \psi)]} \quad (7b)$$

$$I_1 = [a_1 + M_1 (I_2/I_1)^{1/2} \cos(\phi + \psi)] / \beta_1 \quad (7c)$$

$$I_2 = (I_2/I_1) I_1 \quad (7d)$$

TABLE I. Coefficients that define gain medium saturation from Ref. 2

Coefficient	Homogeneous Medium	Inhomogeneous Medium
a_n	$\mathcal{L}F_{1,n} - F_{2,n}$	$e^{-\zeta^2} F_{1,n} - F_{2,n}$
β_n	$\mathcal{L}^2 F_{3,n}$	$(1 + \mathcal{L}) F_{3,n}$
σ_n	$\xi \mathcal{L} F_{1,n}$	$2 F_{1,n} D(\zeta)$
ρ_n	$\xi \beta_n$	$\xi \mathcal{L} F_{3,n}$

$$F_{1,n} = (g_{00} \ell / t_r)_n \quad (g \equiv d \ln I / dx)$$

$$F_{2,n} = (g_c \ell / t_r)_n$$

$$F_{3,n} = F_{1,n} \text{ (assumes } I \text{ normalized by saturation value)}$$

$$\xi = (\omega - \nu) / \gamma$$

$$\mathcal{L} = (1 + \xi^2)^{-1}$$

$$\zeta = (\gamma / \gamma_d) \xi$$

$$D(\zeta) = \text{Dawson integral} = e^{-\zeta^2} \int_0^{\zeta} e^{x^2} dx$$

$$g_{00} = \text{line center - zero power - gain}$$

$$g_c = \text{threshold gain} = - \ln(R_{11} R)^{1/2} / \ell$$

$$\ell = \text{length of gain region}$$

$$\begin{aligned} \gamma\Delta = & \sigma_2 - \sigma_1 + \rho_1 I_1 - \rho_2 I_2 - M_2 (I_1/I_2)^{1/2} \sin(\phi - \psi) \\ & - M_1 (I_2/I_1)^{1/2} \sin(\phi + \psi) \end{aligned} \quad (7e)$$

$$\Delta_2 = \Delta + \Delta_1 \quad (7f)$$

The procedure for obtaining a solution is as follows.

The quantities ϕ , ψ , M_1 , M_2 , Δ_1 , γ , $F_{1,n}$, $F_{2,n}$ and $F_{3,n}$ are specified. For an inhomogeneous medium, the doppler half width γ_d is also specified. The value of ξ is estimated and I_1/I_2 is obtained from Eq. (7a). A new estimate for ξ is then obtained from Eq. (7b). The procedure is repeated until the estimate for ξ converges. The quantities I_1 , I_2 , Δ , and Δ_2 are then found from Eqs. (7c) through (7f). The variables ψ , M_1 , M_2 , Δ_1 , Δ_2 , γ , $F_{1,n}$, $F_{2,n}$, and $F_{3,n}$ are resonator and gain medium properties. The above procedure provides the corresponding values of laser frequency ν , phase angle ϕ , and laser intensities I_1 and I_2 . Equation (7a) is fourth order in $(I_1/I_2)^{1/2}$ so that four steady-state solutions for $(I_1/I_2)^{1/2}$ are possible, in principle. However, in all cases considered herein, no more than one stable steady-state solution has been found for a given set of initial conditions. Stability is examined in the next section.

D. STABILITY CRITERION

The stability of the steady-state solutions can be determined by considering the effect of small perturbations.

Let $E_1 = E_{10} + \Delta E_1$, $E_2 = E_{20} + \Delta E_2$, and $\phi = \phi_0 + \Delta\phi$ where subscript zero denotes the steady-state solution and $\Delta()$ denotes an unsteady perturbation.

Substitution into Eqs. (5a), (5b), and (5e) and neglect of terms of order Δ^2 then yields

$$\begin{pmatrix} \Delta \dot{E}_1 \\ \Delta \dot{E}_2 \\ E_{10} \Delta \dot{\phi} \end{pmatrix} = \begin{pmatrix} a_{11} & a_{12} & a_{13} \\ a_{21} & a_{22} & a_{23} \\ a_{31} & a_{32} & a_{33} \end{pmatrix} \begin{pmatrix} \Delta E_1 \\ \Delta E_2 \\ E_{10} \Delta \phi \end{pmatrix} \quad (8)$$

where

$$a_{11} = a_1 - 3\beta_1 I_{10}$$

$$a_{12} = M_1 \cos(\phi_0 + \psi)$$

$$a_{13} = -M_1 (E_{20}/E_{10}) \sin(\phi_0 + \psi)$$

$$a_{21} = M_2 \cos(\phi_0 - \psi)$$

$$a_{22} = a_2 - 3\beta_2 I_{20}$$

$$a_{23} = -M_2 \sin(\phi_0 - \psi)$$

$$a_{31} = 2\rho_1 I_{10} - M_2 (E_{10}/E_{20}) \sin(\phi_0 - \psi) + M_1 (E_{20}/E_{10}) \sin(\phi_0 + \psi)$$

$$a_{32} = -2\rho_2 E_{10} E_{20} + M_2 (I_{10}/I_{20}) \sin(\phi_0 - \psi) - M_1 \sin(\phi_0 + \psi)$$

$$a_{33} = -M_2 (E_{10}/E_{20}) \cos(\phi_0 - \psi) - M_1 (E_{20}/E_{10}) \cos(\phi_0 + \psi)$$

In the limit $\psi = -\pi/2$, these equations agree with corresponding equations in Ref. 1. Perturbations are damped, and the system is stable, if the roots of the characteristic equation

$$|a_{ij} - \delta_{ij}r| = 0 \quad (10)$$

have negative real parts.

E. SIMILITUDE

The steady-state equations depend on ϕ and ψ through terms of the form $\cos(\phi \pm \psi)$ and $\sin(\phi \pm \psi)$. Equivalent cases are now noted. Let $f(\phi, \psi)$ denote a dependent variable. Equations (7a) through (7f) indicate

$$f(\phi \pm \pi, \psi \pm \pi) = f(\phi, \psi) \quad (11)$$

For the special case $\Delta_1 = 0$,

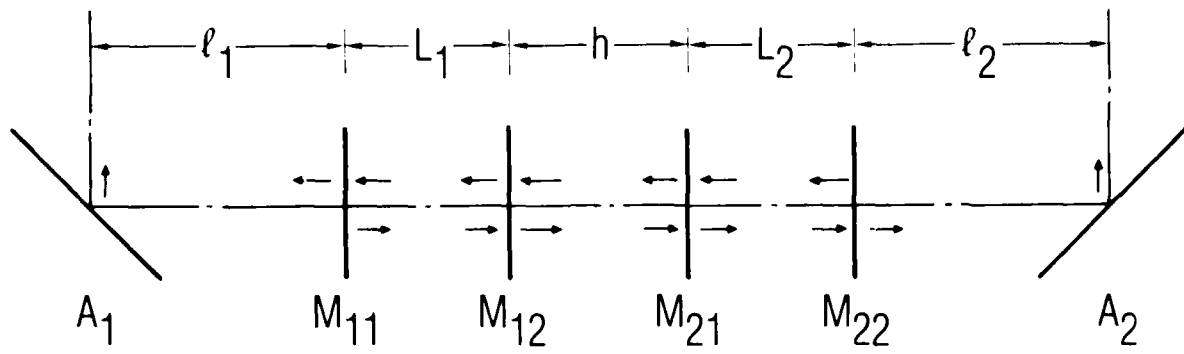
$$f(-\phi, -\psi) = f(\phi, \psi) \quad f = I_1, I_2 \quad (12a)$$

$$= -f(\phi, \psi) \quad f = \xi, \Delta, \tilde{\phi} \quad (12b)$$

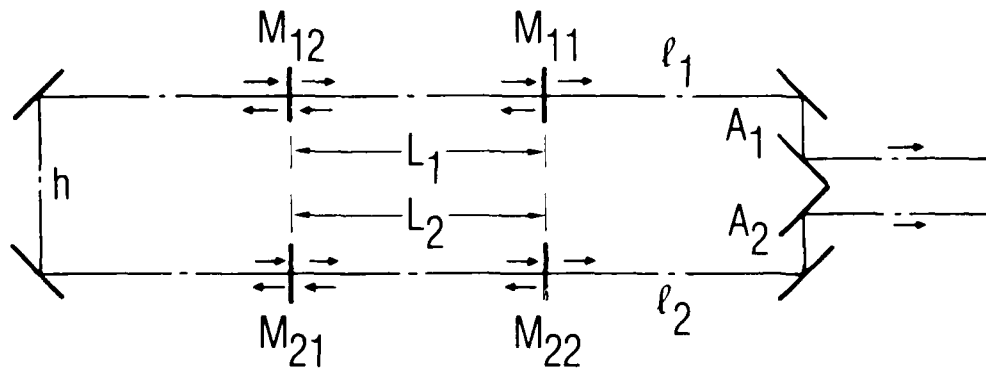
where $\tilde{\phi}$ is defined in Eq. (15).

F. BEAM COMBINATION

The output from each of the coupled resonators can be directed to antennae which are either separated (Fig. 3a) or collocated (Fig. 3b). When a coupled resonator is operating under steady state conditions (i.e., lock in),



(a) PHASED ARRAY



(b) BEAM COMBINER

Fig. 3. Applications of coupled resonator output.

the configuration in Fig. 3a constitutes a phased array while the configuration in Fig. 3b constitutes a technique for coherent beam combination. Factors affecting the beam quality of the latter configuration are discussed herein for both single line and multiline coupled resonators.

The beam quality of the output beam indicated in Fig. 3b can be expressed

$$BQ \equiv I_{\text{ideal}}/I_{\text{actual}} \quad (13)$$

where I_{actual} is far-field center line intensity and I_{ideal} is the value for a combined beam with uniform near-field phase and intensity. Values of beam quality above 1 indicate a lack of near-field phase uniformity. Assume that the output beams from the resonators in Fig. 3b are equal in area and intensity and illuminate subapertures (A_1 and A_2) of equal area. Let ϕ_{A_1} and ϕ_{A_2} denote the phase of the radiation at A_1 and A_2 , respectively, and assume $(\phi_{A_2} - \phi_{A_1})^2 \ll 1$. The beam quality of the combined beam is then³

$$BQ - 1 = \left(\frac{\phi_{A_2} - \phi_{A_1}}{2} \right)^2 + O(\phi_{A_2} - \phi_{A_1})^4 \quad (14)$$

Equation (14) can be evaluated as a function of coupled resonator geometry and gain medium properties.

For a single line stable coupled resonator the phase of the output beam at stations M_{11} and A_1 can be shown to be $\phi_1 + (\Delta\phi_1/2)$ and $\phi_1 + (\Delta\phi_1/2) - k\ell_1$, respectively, where $k = 2\pi/\lambda$. Similarly, the phase of the output beam at M_{22} and A_2 is $\phi_2 + (\Delta\phi_2/2)$ and $\phi_2 + (\Delta\phi_2/2) - k\ell_2$, respectively. The phase difference between the radiation at A_2 and A_1 is then

$$\phi_{A_2} - \phi_{A_1} = \phi + \left(\frac{T}{R}\right)^{1/2} \tilde{\phi} - k(\ell_2 - \ell_1) \quad (15a)$$

where $\phi \equiv \phi_2 - \phi_1$ and

$$\tilde{\phi} \equiv \frac{\Delta\phi_2 - \Delta\phi_1}{2(T/R)^{1/2}} = -\frac{1}{2} \left[\frac{E_1}{E_2} \sin(\phi - \psi) + \frac{E_2}{E_1} \sin(\phi + \psi) \right] \quad (15b)$$

$$= -\sin \phi \sin \psi \quad (E_1 = E_2) \quad (15c)$$

Substitution of Eq. (15a) into Eq. (14) defines the beam quality of the combined beam. In a single-line stable resonator, with $L_1 \neq L_2$, it can be shown that $\phi \neq 0$. However, the condition $\phi_{A_2} - \phi_{A_1} = 0$ (i.e., good beam quality) can be achieved by proper choice of $\ell_2 - \ell_1$ in Eq. (15a). In a multiline stable coupled resonator, with $L_1 \neq L_2$, however, the values of k , ϕ , and $\tilde{\phi}$ differ for each wavelength. Hence, it is not possible to adjust $\ell_2 - \ell_1$ so as to obtain good beam quality for all wavelengths. Therefore, a necessary condition to achieve good beam quality, for the case of a multiline stable coupled resonator, is to operate under conditions where $L_1 \doteq L_2$ and $\ell_1 \doteq \ell_2$. In this case ϕ , $\tilde{\phi}$ and $\phi_{A_2} - \phi_{A_1}$ are small for each wavelength and good beam quality is obtained provided the solution is stable.

III. SPECIAL CASES

Numerical methods are generally needed to evaluate coupled resonator performance. Explicit expressions can be obtained in special cases. The cases $\cos(\phi + \psi) = \cos(\phi - \psi)$ and $\phi^2 \ll 1$ are considered here.

A. ASSUMPTIONS

Let $L \equiv (L_1 + L_2)/2$ denote the average length of resonators 1 and 2 and assume

$$(L_2 - L_1)/L = O(\lambda/L) \ll 1 \quad (16a)$$

It follows that

$$t_{r,n} = t_r [1 + O(\lambda/L)] \quad (16b)$$

$$M_n = M[1 + O(\lambda/L)] \quad (16c)$$

where $t_r \equiv 2L/c$ and $M \equiv (T/R)^{1/2}/t_r$. We also assume that the gain medium and the mirror configuration for resonators 1 and 2 are nominally identical. We therefore replace M_n , a_n , β_n , σ_n , and ρ_n in Eqs. (5) and (7) by the mean values M , a , β , σ , and ρ . Under these conditions the dependent variables

$$I_1, I_2, \xi, \phi \quad (17)$$

are functions of the parameters

$$\psi, \frac{M}{F_2}, \frac{F_1}{F_2}, \Delta_1, \Delta_2, \frac{\gamma}{F_2}, \frac{\gamma}{\gamma_d} \quad (18)$$

To facilitate computations, ϕ is sometimes specified and the corresponding value of Δ_1 (or Δ_2) is determined.

B. CASE $\cos(\phi + \psi) = \cos(\phi - \psi)$

To simplify Eq. (7a), we assume that ϕ and ψ satisfy the relation

$$\cos(\phi + \psi) = \cos(\phi - \psi) \equiv \cos\phi \cos\psi \quad (19)$$

Equation (19) is equivalent to $\sin\phi \sin\psi = 0$ and is satisfied by

$$\phi = 0, \pi; \psi = \text{arbitrary} \quad (20a)$$

and by

$$\psi = 0, \pi; \phi = \text{arbitrary} \quad (20b)$$

Equation (20a) includes the case where $L_1 = L_2$ and h is variable.

Equation (20b) includes the case where $L_1 \neq L_2$ and kh has a value equal to an integral number of half wave lengths. Substitution of Eq. (19) into Eq. (7) yields

$$(I_1/I_2)^{1/2} = 1 \quad (21a)$$

$$= \frac{-1 \pm (1-4D^2)^{1/2}}{2D} \quad (21b)$$

where

$$D = (M/a) \cos\phi \cos\psi \quad (21c)$$

and the root $(I_1/I_2)^{1/2} = -1$ has been omitted. Equation (21b) provides real positive solutions when $-\frac{1}{2} < D < 0$. Several numerical examples, however, indicate that these solutions are unstable. We therefore pursue the case $I_1 = I_2 = 1$. Substitution of the latter relation into Eq. (7) yields

$$\xi = \frac{\gamma\Delta_1 - M \sin(\phi + \psi)}{\gamma + (\sigma/\xi) - [\rho/(\xi\beta)][a + M \cos(\phi + \psi)]} \quad (22a)$$

$$= \frac{\gamma\Delta_1 - M \sin(\phi + \psi)}{\gamma + F_2 - M \cos(\phi + \psi)} \quad \begin{array}{l} \text{homogeneous} \\ \text{medium} \end{array} \quad (22b)$$

$$I = [a + M \cos(\phi + \psi)]/\beta \quad (22c)$$

$$\gamma\Delta = -2M \sin\phi \cos\psi \quad (22d)$$

$$\tilde{\phi} = 0 \quad (22e)$$

Equations (22a) through (22e) provide a solution for ξ , I , and Δ when γ , Δ_1 , M , ϕ , ψ , F_1 , and F_2 are specified.

When $\psi = 0, \pi$ and ϕ is arbitrary the roots of Eq. (10) are

$$r_1 = -2M \cos \phi \cos \psi \quad (23a)$$

$$r_2 = r_1 - 2a \quad (23b)$$

$$r_3 = 2r_1 - 2a \quad (23c)$$

The coupled resonator solution is stable when $r_1 < 0$ or

$$-\pi/2 < \phi < \pi/2 \quad \psi = 0 \quad (24a)$$

$$\pi/2 < \phi < 3\pi/2 \quad \psi = \pi \quad (24b)$$

Note the identity

$$\frac{\Omega_2 - \Omega_1}{2\pi (c/2L)} \equiv \frac{L_1 - L_2}{\lambda/2} \equiv \frac{-Y\Delta(T/R)^{1/2}}{2\pi M} \quad (25)$$

It follows, from Eqs. (22d), (24), and (25) that the tuning range for stable operation is

$$\frac{|L_1 - L_2|}{\lambda/2} < \frac{1}{\pi} \left(\frac{T}{R}\right)^{1/2} \quad (26)$$

The tuning range increases linearly with $(T/R)^{1/2}$.

Similarly, when $\phi = 0, \pi$ and ψ is arbitrary the roots of Eq. (10) are

$$r_1 = -2(2a + b)/3 \quad (27a)$$

$$r_{2,3} = -b \pm (b^2 - 4c)^{1/2} \quad (27b)$$

where

$$b = a + 3M \cos\phi \cos\psi \quad (27c)$$

$$c = M^2(1 + \cos^2 \psi) + M \cos\phi(a \cos\psi + \rho I \sin\psi) \quad (27d)$$

Consideration of the root r_2 indicates that the system is stable when the conditions $b > 0$ and $c > 0$ are satisfied. The condition $b > 0$ is satisfied by

$$\cos\psi > -\frac{a}{3M} \quad \phi = 0 \quad (28a)$$

$$\cos\psi < \frac{a}{3M} \quad \phi = \pi \quad (28b)$$

In the limit $(a/3M)^3 \ll 1$, the latter stability region becomes

$$|\psi| < \frac{\pi}{2} + \frac{a}{3M} + O\left(\frac{a}{3M}\right)^3 \quad \phi = 0 \quad (29a)$$

$$\pi > |\psi| > \frac{\pi}{2} - \frac{a}{3M} + O\left(\frac{a}{3M}\right)^3 \quad \phi = \pi \quad (29b)$$

The condition $c > 0$ is satisfied by

$$\cos\phi \cos\psi > -\frac{M}{a} (1 + \cos^2 \psi) - \frac{\rho I}{a} \sin\psi \cos\phi \quad (30)$$

For a homogeneous medium with $\phi = \Delta_1 = 0$, Eq. (30) becomes

$$\cos \psi > \frac{M}{\gamma + F_2} \frac{1 - (\gamma + F_2)(1 + \cos^2 \psi)/a}{1 - 2M^2/[a(\gamma + F_2)]} \quad (31a)$$

$$> \frac{M}{\gamma + F_2} \left[1 + O\left(\frac{\gamma + F_2}{a}\right) + O\left(\frac{M^2}{a(\gamma + F_2)}\right) \right] \quad (31b)$$

When $a/3M$ is small, values of ψ for stable operation are determined by the condition $b > 0$. When $a/3M$ is large, values of ψ for stable operation are determined by the condition $c > 0$. The range of ψ for stable operation first increases and then decreases with increase in a/M (Fig. 4). In cases where $\xi^2 \ll 1$, the substitution $a = F_1 - F_2$ simplifies the evaluation of stability.

C. CASE $\phi^2 \ll 1$

We assume $\phi^2 \ll 1$ and express dependent variables in the form

$$E_1/E_2 = 1 + \phi E_{11} \quad (32a)$$

$$a = a_0(1 + \phi a_{11}) \quad (32b)$$

$$\beta = \beta_0(1 + \phi \beta_{11}) \quad (32c)$$

where subscript zero denotes values for $\phi = 0$ and where a_{11} is not to be confused with Eq. (9a). Substitution into Eqs. (7a) through (7f) and neglect of terms of order ϕ^2 yields

$$E_{11} = \frac{-A}{1 + 2A} \tan \psi \quad (33a)$$

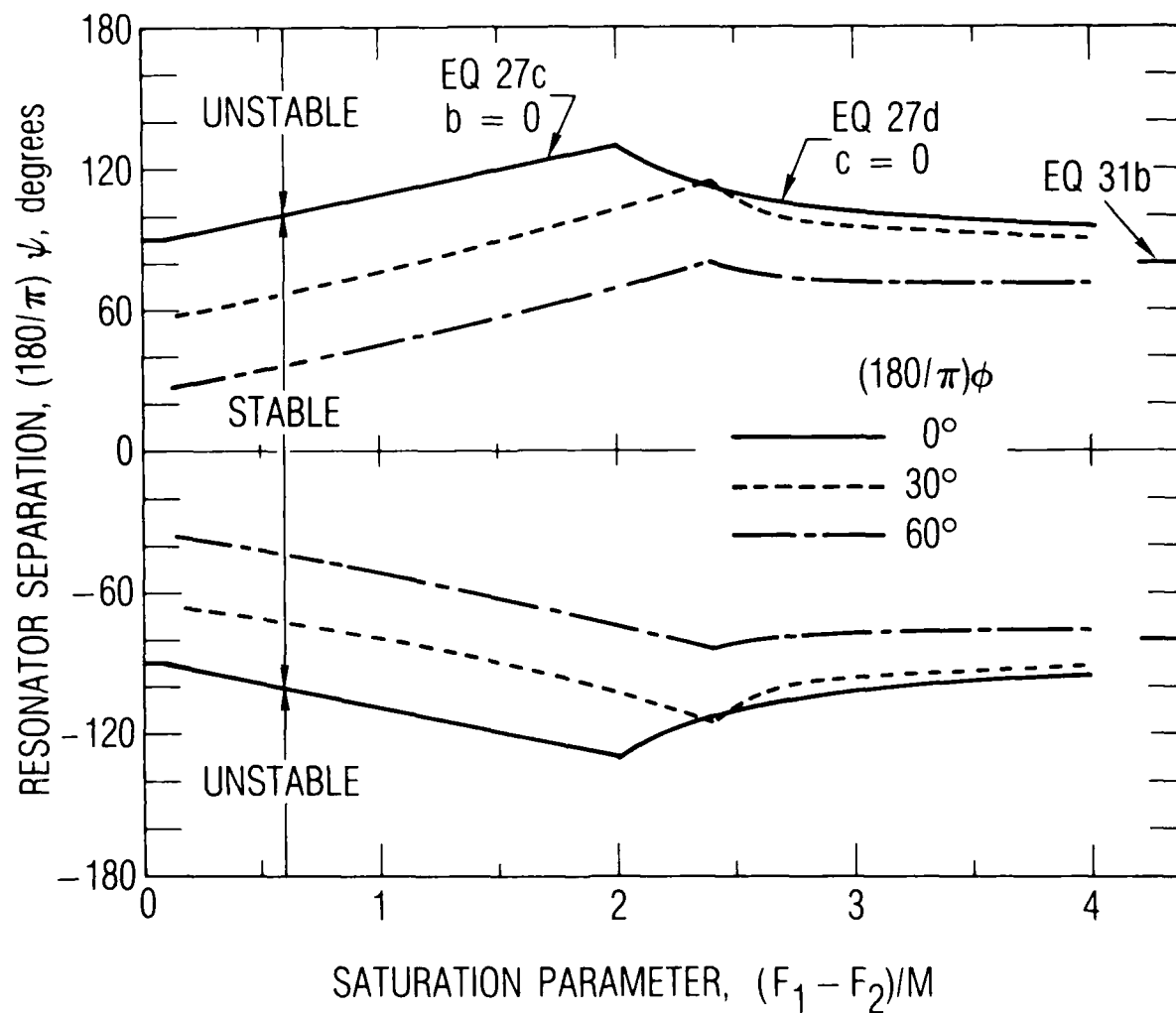


Fig. 4. Effect of saturation on range of ψ for stable operation. A homogeneous medium is assumed with input conditions given in Table II.

$$\frac{Y\Delta}{2\phi} = E_{11} \left[\frac{\rho_o a_o}{\beta_o} (1+A) + M \sin\psi \right] - M \cos\psi \quad (33b)$$

$$\tilde{\phi} = -\phi(\cos\psi - E_{11} \sin\psi) \quad (33c)$$

where

$$A \equiv (M/a_o)\cos\psi$$

Equation (33a) indicates the departure from the condition $I_1/I_2 = 1$ as ϕ is increased from zero. Equation (33b) indicates the relation between ϕ and the tuning parameter Δ . Additional expressions for dependent variables can be readily obtained.

IV. RESULTS AND DISCUSSION

The effect of variations in ϕ and ψ on steady-state coupled resonator performance has been evaluated for initial conditions given in Table II. Calculations were conducted at intervals of $\Delta\phi = \Delta\psi = 2^\circ$. The results are given in Tables III and IV for homogeneous and inhomogeneous media, respectively, and are discussed herein. The end of each stable operating regime, denoted by an asterisk in Tables III and IV, is correct to within 2° due to the computational interval.

A. ϕ FIXED AND ψ VARIED

The present computations correspond to keeping $L_1(\Delta_1 = 0)$ and $L_2(\Delta_2 \sim \phi)$ fixed while varying $h(\psi)$.

The net output is proportional to $I_1 + I_2$ and is a maximum when $\phi = \psi = 0$. When $\phi = 0$, an increase in $|\psi|$ results in a decrease in net output and stable operation is limited to the range $-96^\circ < \psi < 96^\circ$. With increase in ϕ the peak output continues to occur at $\psi = 0$ (except when $\phi = 90^\circ$) but is reduced from the output at $\phi = \psi = 0$. The range of ψ for stable operation is also reduced with increase in ϕ .

The data in Tables III and IV correspond to a fixed degree of saturation, F_1/F_2 . The effect of this parameter on the range of ψ for stable operation is indicated in Fig. 4 where stability limits are plotted versus $(F_1 - F_2)/M$. When $\phi = 0$, the stable operating regime limit increases from $\psi = \pm 90^\circ$ at $(F_1 - F_2)/M = 0$ (threshold) to $\psi = \pm 130^\circ$ at $(F_1 - F_2)/M = 2$. These results can be obtained by taking $b = 0$ in Eq. (27c). The range of ψ for stable operation decreases with further increase in $(F_1 - F_2)/M$ and is deduced by taking $c = 0$ in Eq. (27d). An increase in ϕ results in a decrease in the

TABLE II. Input for numerical computations

γ	$= 0.50 \times 10^8 \text{ rad/s}$
γ_d	$= 1.00 \times 10^9 \text{ rad/s (Table IV)}$
M	$= 0.10 \times 10^8 \text{ s}^{-1}$
F_1	$= 0.20 \times 10^8 \text{ s}^{-1}$
	$= 0.17 \times 10^8 - 0.60 \times 10^8 \text{ s}^{-1} \text{ (Fig. 4)}$
F_2	$= 0.16 \times 10^8 \text{ s}^{-1}$
Δ_1	$= 0$

TABLE III. Coupled resonator performance for case of homogeneous medium. Input conditions given in Table II. Asterisk denotes end of stable operating regime to within 2°.

(a) ϕ Fixed and ψ Varied						
$\frac{180}{\pi} \phi$	$\frac{180}{\pi} \psi$	ξ	I_1	I_2	I_1+I_2	Δ_2
0	0	0.000	0.700	0.700	1.400	0.000
	± 30	∓ 0.087	0.635	0.635	1.270	0.000
	± 60	∓ 0.142	0.448	0.448	0.896	0.000
	± 90	∓ 0.152	0.186	0.186	0.372	0.000
	$\pm 96^*$	∓ 0.148	0.132	0.132	0.264	0.000
30	-114^*	0.153	0.240	0.239	0.479	0.081
	-90	0.091	0.362	0.156	0.518	-0.143
	-60	0.053	0.479	0.198	0.677	-0.240
	-30	0.000	0.637	0.486	1.123	-0.198
	0	-0.087	0.635	0.635	1.270	-0.200
	30	-0.165	0.486	0.642	1.128	-0.189
	60	-0.256	0.157	0.448	0.605	-0.252
	62^*	-0.298	0.099	0.393	0.492	-0.315
60	-90^*	0.066	0.539	0.331	0.870	-0.044
	-60	0.000	0.497	0.176	0.673	-0.291
	-30	-0.053	0.479	0.198	0.677	-0.381
	0	-0.142	0.448	0.448	0.896	-0.346
	30	-0.256	0.157	0.448	0.605	-0.371
	32^*	-0.309	0.093	0.393	0.486	-0.426
90	$-6^*/186^*$	∓ 0.109	0.231	0.118	0.349	∓ 0.425
	$-4/184$	∓ 0.124	0.220	0.146	0.366	∓ 0.411
	$-2/182$	∓ 0.138	0.205	0.168	0.373	∓ 0.404
	0/180	∓ 0.152	0.186	0.186	0.372	∓ 0.400
	2/178	∓ 0.167	0.162	0.199	0.361	∓ 0.400
	$4^*/176^*$	∓ 0.188	0.131	0.208	0.339	∓ 0.404

TABLE III. Coupled resonator performance for case of homogeneous medium. Input conditions given in Table II. Asterisk denotes end of stable operating regime to within 2° (Continued).

(b) ψ Fixed and ϕ Varied						
$\frac{180}{\pi} \psi$	$\frac{180}{\pi} \phi$	ξ	I_1	I_2	I_1+I_2	Δ_2
0	0	0.000	0.700	0.700	1.400	0.000
	± 30	∓ 0.087	0.635	0.635	1.270	∓ 0.200
	± 60	∓ 0.142	0.448	0.448	0.896	∓ 0.346
	$\pm 90^*$	∓ 0.152	0.186	0.186	0.372	∓ 0.400
30	-92^*	0.096	0.357	0.166	0.523	0.376
	-90	0.091	0.362	0.156	0.518	0.385
	-60	0.053	0.479	0.198	0.677	0.381
	-30	0.000	0.637	0.486	1.123	0.198
	0	-0.087	0.635	0.635	1.270	0.000
	30	-0.165	0.486	0.642	1.128	-0.189
	60	-0.256	0.157	0.448	0.605	-0.371
	62^*	-0.298	0.099	0.393	0.492	-0.422
60	-144^*	0.164	0.242	0.277	0.519	0.134
	-140	0.159	0.279	0.298	0.577	0.136
	-130^*	0.145	0.360	0.338	0.698	0.148
	-74^*	0.028	0.538	0.261	0.799	0.243
	-60	0.000	0.497	0.176	0.673	0.291
	-30	-0.053	0.479	0.198	0.677	0.240
	0	-0.142	0.448	0.448	0.896	0.000
	30	-0.256	0.157	0.448	0.605	-0.252
	32^*	-0.309	0.093	0.393	0.486	-0.335
	$-60^*/240^*$	∓ 0.066	0.539	0.331	0.870	± 0.044
	$-50/230$	∓ 0.081	0.491	0.283	0.774	± 0.065
	$-40/220$	∓ 0.090	0.431	0.224	0.655	± 0.095
90	$-30/210$	∓ 0.091	0.362	0.156	0.518	± 0.143
	$-22/202$	∓ 0.083	0.304	0.099	0.403	± 0.213
	$-10/190$	∓ 0.142	0.271	0.232	0.503	± 0.028
	0/180	∓ 0.152	0.186	0.186	0.372	0.000
	$4^*/176^*$	∓ 0.188	0.131	0.208	0.339	∓ 0.088

TABLE IV. Coupled resonator performance for case of inhomogeneous medium. Input conditions given in Table II. Asterisk denotes end of stable operating regime to within 2°.

(a) ϕ Fixed and ψ Varied						
$\frac{180}{\pi} \phi$	$\frac{180}{\pi} \psi$	ξ	I_1	I_2	I_1+I_2	Δ_2
0	0	0.000	0.350	0.350	0.700	0.000
	± 30	∓ 0.109	0.318	0.318	0.636	0.000
	± 60	∓ 0.182	0.229	0.229	0.458	0.000
	± 90	∓ 0.200	0.102	0.102	0.204	0.000
	$\pm 96^*$	∓ 0.197	0.075	0.075	0.150	0.000
30	-112^*	0.183	0.134	0.112	0.246	0.048
	-90	0.115	0.182	0.075	0.257	-0.152
	-60	0.068	0.240	0.100	0.340	-0.241
	-30	0.000	0.318	0.243	0.561	-0.198
	0	-0.109	0.318	0.318	0.636	-0.200
	30	-0.210	0.248	0.325	0.573	-0.192
	60	-0.309	0.104	0.251	0.355	-0.229
	68^*	-0.440	0.022	0.114	0.136	-0.387
60	-90^*	0.083	0.269	0.163	0.432	-0.047
	-60	0.000	0.249	0.088	0.337	-0.291
	-30	-0.068	0.240	0.100	0.340	-0.378
	0	-0.182	0.229	0.229	0.458	-0.346
	30	-0.309	0.104	0.251	0.355	-0.358
	38^*	-0.449	0.020	0.109	0.129	-0.483
90	$-34^*/214^*$	∓ 0.116	0.196	0.089	0.285	∓ 0.362
	-30/210	∓ 0.115	0.182	0.075	0.257	∓ 0.385
	-10/190	∓ 0.150	0.134	0.075	0.209	∓ 0.414
	0/180	∓ 0.200	0.102	0.102	0.204	∓ 0.400
	$6^*/174^*$	∓ 0.267	0.067	0.123	0.190	∓ 0.411

TABLE IV. Coupled resonator performance for case of inhomogeneous medium. Input conditions given in Table II. Asterisk denotes end of stable operating regime to within 2° (Continued).

(a) ϕ Fixed and ψ Varied						
$\frac{180}{\pi} \psi$	$\frac{180}{\pi} \phi$	ξ	I_1	I_2	I_1+I_2	Δ_2
0	0	0.000	0.350	0.350	0.700	0.000
	± 30	∓ 0.109	0.318	0.318	1.636	∓ 0.200
	± 60	∓ 0.182	0.229	0.229	0.458	∓ 0.346
	$\pm 90^*$	∓ 0.200	0.102	0.102	0.204	∓ 0.400
30	-92^*	0.122	0.180	0.080	0.260	0.376
	-90	0.115	0.182	0.075	0.257	0.385
	-60	0.068	0.240	0.100	0.340	0.378
	-30	0.000	0.318	0.243	0.561	0.198
	0	-0.109	0.318	0.318	0.638	0.000
	30	-0.210	0.248	0.325	0.573	-0.192
	60	-0.309	0.104	0.251	0.355	-0.358
	68	-0.440	0.022	0.114	0.136	-0.494
60	-142^*	0.199	0.137	0.135	0.272	0.122
	-140	0.197	0.145	0.140	0.285	0.124
	-130^*	0.182	0.183	0.161	0.344	0.141
	-74^*	0.036	0.269	0.130	0.399	0.242
	-60	0.000	0.249	0.088	0.337	0.291
	-30	-0.068	0.240	0.100	0.340	0.241
	0	-0.182	0.229	0.229	0.458	0.000
	30	-0.309	0.104	0.251	0.355	-0.229
	38^*	-0.449	0.020	0.109	0.129	-0.419
	$-60^*/240^*$	∓ 0.083	0.269	0.163	0.432	± 0.047
	-50/230	∓ 0.103	0.245	0.139	0.384	± 0.070
	-40/220	∓ 0.114	0.216	0.109	0.325	± 0.102
90	-30/210	∓ 0.115	0.182	0.075	0.257	± 0.152
	-10/190	∓ 0.150	0.134	0.075	0.209	± 0.111
	0/180	∓ 0.200	0.102	0.102	0.204	0.000
	$8^*/172^*$	∓ 0.340	0.041	0.126	0.167	∓ 0.226

stable operating range for ψ . In all cases the range of ψ for stable operation is approximately $\pm 90^\circ$ which corresponds to maintaining control of h to within half a wavelength.

B. ψ FIXED AND ϕ VARIED

The present computations correspond to keeping $L_1(\Delta_1 = 0)$ and $h(\psi)$ fixed while varying $L_2(\Delta_2 \sim \phi)$. Peak power occurs at $\phi = \psi = 0$ and for $\psi \neq 0$, has a local maximum at $\phi = 0$. The results for $\psi = 0$ agree with Eqs. (23) through (26) and indicate a stable range

$$-\frac{1}{\pi} \left(\frac{T}{R} \right)^{1/2} < \frac{L_1 - L_2}{\lambda/2} < \frac{1}{\pi} \left(\frac{T}{R} \right)^{1/2} \quad (34)$$

The range of Δ_2 and therefore of $(L_1 - L_2)/\lambda$ for stable operation decreases as ψ increases. Tables IIIb and IVb indicate that when $\psi \neq 0$, the solution, in some cases, is a multivalued function of Δ_2 . The impact on coupled laser performance has not been pursued.

C. GAIN MEDIUM EFFECTS

The performance of coupled lasers with homogeneous and inhomogeneous gain mediums are compared in Tables III and IV, respectively. Initial conditions of Table II are used. It is seen that for these initial conditions the range of stable operation and the dependence of output power on ϕ and ψ is insensitive to the nature of the gain medium. [The factor two difference in I between Tables III and IV is a gain medium property and is not significant.] However, this good agreement may not apply for initial conditions which yield ξ^2 not small.

V. MULTILINE COUPLED RESONATOR PERFORMANCE

The previous results have assumed a single lasing transition. We now consider the effect of multiline operation. To achieve good beam quality it is necessary to operate under conditions such that $\phi = 0$ as noted in Eq. (15). The stability of this configuration requires consideration.

We first consider a homogeneous gain medium with a single longitudinal mode for each laser line. Let λ_p and λ_q denote the smallest and largest wavelengths, in the multiline coupled resonator, and let λ denote a mean value. If a lossy etalon is assumed, the corresponding values of ψ are $\psi_p = 2\pi h/\lambda_p$ and $\psi_q = 2\pi h/\lambda_q$. Consider a typical device wherein $(\lambda_q - \lambda_p)/\lambda = 0(0.1)$ and $h = 0(1\text{m})$. It follows that

$$\psi_p - \psi_q = 2\pi \frac{h}{\lambda} \left(\frac{\lambda_q - \lambda_p}{\lambda} \right) \quad (35a)$$

$$= 0(10^5) \quad (35b)$$

It may be concluded that ψ_p and ψ_q are uncorrelated and the value of ψ , for each wavelength, is random within the interval $-\pi < \psi < \pi$. Since stable operation is limited to the interval $-\pi/2 \lesssim \psi \lesssim \pi/2$ (e.g., Fig. 4) it follows that for any fixed value of h , and a "lossy" etalon, only about half of the possible laser wavelengths can achieve steady-state operation.

In the case of an inhomogeneously broadened medium, there may be many longitudinal modes associated with each laser line. Let λ_p and λ_q denote the wavelength of adjacent longitudinal modes. Neglect mode pulling and pushing and assume $(T/R)^{1/2} \ll 1$ in Eq. (7b). It follows that $\lambda_q - \lambda_p = \lambda^2/2L$ so that

$$\psi_p - \psi_q = \pi h/L \quad (36)$$

In the limit $h/L \rightarrow 0, 2, 4, \dots$ all the longitudinal modes, corresponding to a given laser line, have the same degree of stability or instability. In the limit $h/L \rightarrow 1, 3, 5, \dots$, in general, one longitudinal mode will be stable while the adjacent mode will be unstable. In the latter case, half of the longitudinal modes, for a given line, are stable while the remaining modes are unstable.

The net power and stability of the output from multiline coupled lasers will depend on the competition, if any, between the stable and unstable resonator modes. It is seen from the coupling terms in Eqs. (5a) and (5b) that when $|\phi \pm \psi| < \pi/2$ the stable modes have, in effect, more gain than the corresponding unstable (i.e., uncoupled) modes. Hence, when both the stable and unstable modes compete for the same gain medium, the stable modes will dominate. In the latter case, multiline coupled lasers will tend to provide stable output on a reduced number of lines with relatively little loss in net output power.

VI. CONCLUDING REMARKS

The present study has considered coupled Fabry-Perot resonators with intercavity losses such that $\psi = 2\pi h/\lambda$. In more complex resonator geometries (e.g., hole-coupled and edge-coupled unstable resonators), the radiation generally makes a single pass in the intercavity region. Hence, a phase change relation similar to $\psi = 2\pi h/\lambda$, as well as present results, are expected to be applicable for these devices.

VIII. REFERENCES

1. M. B. Spencer and W. E. Lamb, Jr., "Theory of Two Coupled Lasers," Phys. Rev. A, 5, 893 (1972).
2. M. Sargent III, M. O. Scully and W. E. Lamb Jr., Laser Physics (Addison Wesley, Reading, Mass., 1974), pp. 108,153.
3. M. Born and E. Wolf, Principles of Optics, 4th ed. (Pergamon, New York, 1970), pp. 41,325,464.

APPENDIX

ETALON PERFORMANCE

Mirrors M_{12} and M_{21} may each be etalons. The combination of M_{12} and M_{21} , then, also forms an etalon. The steady-state performance of these configurations is now noted.

I. SINGLE ETALON

A single etalon (e.g., mirror M_{12}) is illustrated in Fig. A-1a. Following the development in Ref. 3, the reflection and transmission coefficients can be expressed

$$\frac{E_{12}^r}{E_{12}^i} \equiv R_{12}^{1/2} e^{i\phi_{12}^r} = \frac{(1 - e^{i\delta_{12}})r}{1 - r^2 e^{i\delta_{12}}} \quad (\text{A-1a})$$

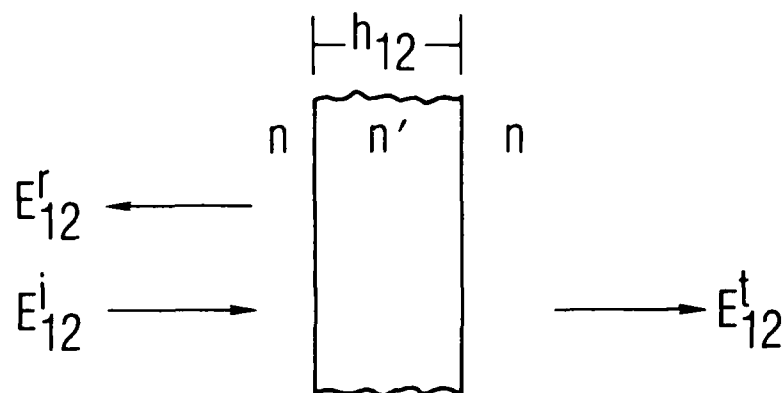
$$\frac{E_{12}^t}{E_{12}^i} \equiv T_{12}^{1/2} e^{i\phi_{12}^t} = \frac{(1 - r^2) e^{i\delta_{12}/2}}{1 - r^2 e^{i\delta_{12}}} \quad (\text{A-1b})$$

where

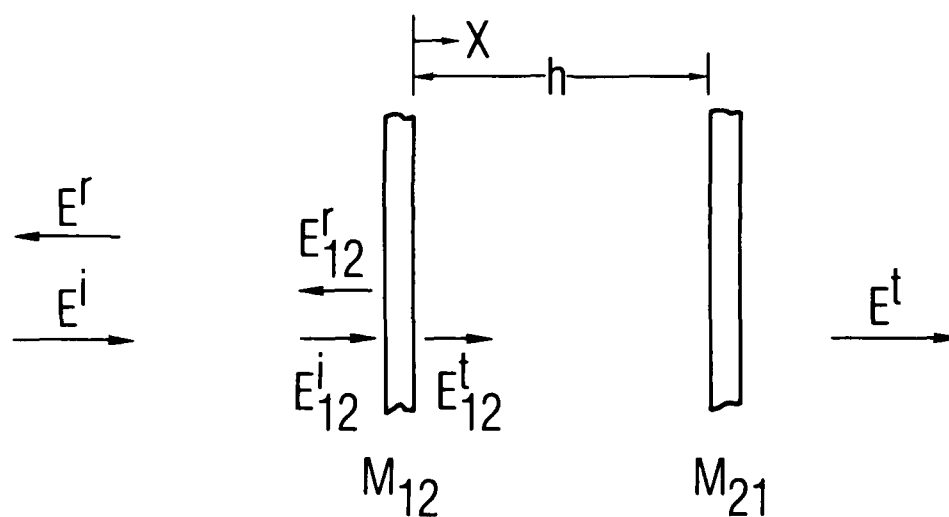
$$r \equiv |(n' - n)/(n' + n)|$$

$$\delta_{12} \equiv 4\pi h_{12}/\lambda_{12}$$

and n, n' denote index of refraction. The coefficient $\exp(i\delta_{12}/2)$ in Eq. (A-1b) is usually neglected³ but is retained here to obtain phase information. Equations (A-1a) and (A-1b) indicate



(a) SINGLE ETALON (mirror M_{12})



(b) DOUBLE ETALON

Fig. A-1a. Etalon configurations.

$$R_{12} = 1 - T_{12} = 4r^2 \sin^2(\delta_{12}/2) / [(1 - r^2)^2 + 4r^2 \sin^2(\delta_{12}/2)] \quad (\text{A-2a})$$

$$\phi_{12}^r = (-1) \tan^{-1} \left[\frac{1 - r^2}{1 + r^2} \cot\left(\frac{\delta_{12}}{2}\right) \right] \quad (\text{A-2b})$$

$$\phi_{12}^t = \tan^{-1} \left[\frac{1 + r^2}{1 - r^2} \tan\left(\frac{\delta_{12}}{2}\right) \right] \quad (\text{A-2c})$$

It follows that

$$\psi_{12} \equiv \phi_{12}^t - \phi_{12}^r = \pm \pi/2 \quad (\text{A-3})$$

II. DOUBLE ETALON

The etalon formed by the combination of mirrors M_{12} and M_{21} is now evaluated. The configuration is illustrated in Fig. A-1b. We assume that scattering losses occur in the space between the mirrors. The local scattering coefficient is taken to be a constant, namely

$$\alpha_s \equiv -d \ln I / dx \equiv -2d \ln E / dx \quad (\text{A-4a})$$

The reduction in electric field intensity, after one round trip, is

$$E_{p+1} / E_p = e^{-\alpha} \quad (\text{A-4b})$$

where $\alpha = \alpha_s h$. The reflection and transmission coefficients for the double etalon, with losses, are then

$$\frac{E^r}{E^i} \equiv R^{1/2} e^{i\phi^r} = R_{12}^{1/2} e^{i\phi_{12}^r} \frac{(1 - e^{-\alpha} e^{i\bar{\delta}})}{1 - R_{12} e^{-\alpha} e^{i\bar{\delta}}} \quad (\text{A-5a})$$

$$\frac{E^t}{E^i} \equiv T^{1/2} e^{i\phi^t} = - \frac{T_{12} e^{-\alpha/2} e^{i(\phi_{12}^r + \bar{\delta}/2)}}{1 - R_{12} e^{-\alpha} e^{i\bar{\delta}}} \quad (\text{A-5b})$$

where

$$\delta = 4\pi h/\lambda$$

$$\bar{\delta} = 2\phi_{12}^r + \delta$$

Equations (A-5a) and (A-5b) indicate

$$R = \frac{R_{12} [(1 - e^{-\alpha})^2 + 4e^{-\alpha} \sin^2(\bar{\delta}/2)]}{(1 - R_{12} e^{-\alpha})^2 + 4e^{-\alpha} R_{12} \sin^2(\bar{\delta}/2)} \quad (\text{A-6a})$$

$$T = \frac{(1 - R_{12})^2 e^{-\alpha}}{(1 - R_{12} e^{-\alpha})^2 + 4e^{-\alpha} R_{12} \sin^2(\bar{\delta}/2)} \quad (\text{A-6b})$$

$$\phi^r = \phi_{12}^r - \tan^{-1} \left[\frac{2(1 - R_{12}) \sin(\bar{\delta}/2) \cos(\bar{\delta}/2)}{e^{\alpha}(1 - R_{12} e^{-\alpha})(1 - e^{-\alpha}) + 2(1 + R_{12}) \sin^2(\bar{\delta}/2)} \right] \quad (\text{A-6c})$$

$$\phi^t = \phi_{12}^r + \tan^{-1} \left[\frac{1 + R_{12} e^{-\alpha}}{1 - R_{12} e^{-\alpha}} \tan\left(\frac{\bar{\delta}}{2}\right) \right] \quad (\text{A-6d})$$

In the present case, $R + T < 1$ when $\alpha > 0$. In the limit $\alpha \rightarrow 0$

$$\psi \equiv \phi^t - \phi^r = \pm \pi/2 \quad (\alpha = 0) \quad (\text{A-7a})$$

This result is consistent with the assumption $\psi = -\pi/2$ used in Ref. 1.

In the limit $\alpha \rightarrow \infty$,

$$\psi = \bar{\delta}/2 \quad (\alpha \rightarrow \infty) \quad (\text{A-7b})$$

In the latter case ψ depends on h/λ .

LABORATORY OPERATIONS

The Aerospace Corporation functions as an "architect-engineer" for national security projects, specializing in advanced military space systems. Providing research support, the corporation's Laboratory Operations conducts experimental and theoretical investigations that focus on the application of scientific and technical advances to such systems. Vital to the success of these investigations is the technical staff's wide-ranging expertise and its ability to stay current with new developments. This expertise is enhanced by a research program aimed at dealing with the many problems associated with rapidly evolving space systems. Contributing their capabilities to the research effort are these individual laboratories:

Aerophysics Laboratory: Launch vehicle and reentry fluid mechanics, heat transfer and flight dynamics; chemical and electric propulsion, propellant chemistry, chemical dynamics, environmental chemistry, trace detection; spacecraft structural mechanics, contamination, thermal and structural control; high temperature thermomechanics, gas kinetics and radiation; cw and pulsed chemical and excimer laser development including chemical kinetics, spectroscopy, optical resonators, beam control, atmospheric propagation, laser effects and countermeasures.

Chemistry and Physics Laboratory: Atmospheric chemical reactions, atmospheric optics, light scattering, state-specific chemical reactions and radiative signatures of missile plumes, sensor out-of-field-of-view rejection, applied laser spectroscopy, laser chemistry, laser optoelectronics, solar cell physics, battery electrochemistry, space vacuum and radiation effects on materials, lubrication and surface phenomena, thermionic emission, photo-sensitive materials and detectors, atomic frequency standards, and environmental chemistry.

Computer Science Laboratory: Program verification, program translation, performance-sensitive system design, distributed architectures for spaceborne computers, fault-tolerant computer systems, artificial intelligence, micro-electronics applications, communication protocols, and computer security.

Electronics Research Laboratory: Microelectronics, solid-state device physics, compound semiconductors, radiation hardening; electro-optics, quantum electronics, solid-state lasers, optical propagation and communications; microwave semiconductor devices, microwave/millimeter wave measurements, diagnostics and radiometry, microwave/millimeter wave thermionic devices; atomic time and frequency standards; antennas, rf systems, electromagnetic propagation phenomena, space communication systems.

Materials Sciences Laboratory: Development of new materials: metals, alloys, ceramics, polymers and their composites, and new forms of carbon; non-destructive evaluation, component failure analysis and reliability; fracture mechanics and stress corrosion; analysis and evaluation of materials at cryogenic and elevated temperatures as well as in space and enemy-induced environments.

Space Sciences Laboratory: Magnetospheric, auroral and cosmic ray physics, wave-particle interactions, magnetospheric plasma waves; atmospheric and ionospheric physics, density and composition of the upper atmosphere, remote sensing using atmospheric radiation; solar physics, infrared astronomy, infrared signature analysis; effects of solar activity, magnetic storms and nuclear explosions on the earth's atmosphere, ionosphere and magnetosphere; effects of electromagnetic and particulate radiations on space systems; space instrumentation.

END

3-87

DTIC